luciferase reporters harboring consensus Bcl6 binding sequences (fig. S5, D and E). Thus, Bcl6 directly associated with and repressed *Men1* transcription in β-cells. Previous studies have shown that steroids like progesterone and dexamethasone can inhibit the mitogenic effects of prolactin on β-cells (*24*), but the underlying mechanism is unknown. Simultaneous exposure of isolated mouse islets to prolactin and progesterone attenuated changes in *Men1*, *p18*, *p27*, and *Bcl6* expression provoked by prolactin alone (Fig. 3, E and F). Thus, multiple hormonal inputs likely regulate β-cell *Men1* expression. Bcl6-dependent changes in *Men1*, *p18*, and *p27* expression provoked by prolactin in MIN6 cells or in cultured human islets (figs. S6 to S8) corroborated these findings and showed that *Men1* regulation by lactogen signaling is evolutionarily conserved.

To test if lactogen signaling was sufficient to reduce *Men1* expression and increase β-cell proliferation in vivo, we transplanted mice with osmotic micropumps to deliver prolactin for 6 days (*25*). Compared with islets from vehicle-infused controls, islets from prolactin-infused mice had a fourfold increase in *Bcl6* expression, a 50% reduction of *Men1*, *p18*, and *p27* mRNA, and a 2.5-fold increase of BrdU incorporation by β-cells (Fig. 3, G to I). Thus, short-term prolactin infusion was sufficient to reduce *Men1* expression in vivo and to stimulate proliferation of adult islet β-cells. Additional studies are needed to determine if lactogenic hormone regulation of *Men1* governs other features that affect β-cell expansion, such as β-cell size and survival (*26*).

To determine if menin might regulate adaptive β-cell expansion in obesity, another common physiological state that stimulates adaptive islet expansion, we measured islet menin levels in A^y mice, a well-characterized model of hyperphagic obesity [reviewed in (*27*)]. At 3 months, when A^y mice are obese but normoglycemic (Fig. 4, A and B), A^y islet levels of *Men1* mRNA, menin, and *p27* and *p18* mRNA and protein were reduced compared to islets from wild-type controls (Fig. 4, C to E). These results suggest that in obesity, menin attenuation regulates adaptive β-cell proliferation.

Studies of endocrine neoplasias in MEN1 syndrome and other cancers have defined menin roles solely in the context of tumor pathogenesis. Our work expands this view, showing that menin functions as a physiological regulator of adaptive β-cell expansion in pregnancy and possibly other common states linked to type 2 diabetes, such as obesity. We speculate that menin may integrate β-cell growth signals in physiological islet expansion, controlling dynamic histone modifications that govern β-cell fate and proliferation. Menin-independent control of maternal β-cell expansion is not excluded by our study, and investigating the role of other islet tumor suppressors, like von Hippel–Lindau protein (*28*), in physiological β-cell expansion might be fruitful. Our finding that *Men1* expression is regulated by prolactin and progesterone raises the possibility that defects in signaling pathways regulated by lactogenic or steroid hormones might underlie specific forms of type 2 diabetes, including gestational diabetes, and endocrine neoplasias linked to

Men1 inactivation, including carcinoid and insulinoma (*7*). Our work also suggests that manipulation of regulators, cofactors, and targets of menin might be a therapeutic strategy for expanding functional pancreatic islets in diabetes.

References and Notes

1. F. A. Van Assche, L. Aerts, F. De Prins, *Br. J. Obstet. Gynaecol.* **85**, 818 (1978).
2. J. A. Parsons, T. C. Brelje, R. L. Sorenson, *Endocrinology* **130**, 1459 (1992).
3. R. L. Sorenson, T. C. Brelje, *Horm. Metab. Res.* **29**, 301 (1997).
4. J. Boloker, S. J. Gertz, R. A. Simmons, *Diabetes* **51**, 1499 (2002).
5. E. Horvath, K. Kovacs, B. W. Scheithauer, *Pituitary* **1**, 169 (1999).
6. C. Larsson, B. Skogseid, K. Oberg, Y. Nakamura, M. Nordenskjold, *Nature* **332**, 85 (1988).
7. S. K. Agarwal *et al.*, *Ann. N. Y. Acad. Sci.* **1014**, 189 (2004).
8. J. J. Heit, S. K. Karnik, S. K. Kim, *Annu. Rev. Cell Dev. Biol.* **22**, 311 (2006).
9. C. M. Hughes *et al.*, *Mol. Cell* **13**, 587 (2004).
10. A. Yokoyama *et al.*, *Mol. Cell. Biol.* **24**, 5639 (2004).
11. S. K. Karnik *et al.*, *Proc. Natl. Acad. Sci. U.S.A.* **102**, 14659 (2005).
12. T. A. Milne *et al.*, *Proc. Natl. Acad. Sci. U.S.A.* **102**, 749 (2005).
13. R. W. Schnepp *et al.*, *Cancer Res.* **66**, 5707 (2006).
14. D. S. Franklin, V. L. Godfrey, D. A. O'Brien, C. Deng, Y. Xiong, *Mol. Cell. Biol.* **20**, 6147 (2000).
15. Materials and methods are available as supporting material on *Science* Online.
16. J. J. Heit *et al.*, *Nature* **443**, 345 (2006).
17. T. C. Brelje *et al.*, *Endocrinology* **132**, 879 (1993).
18. J. H. Nielsen, *Endocrinology* **110**, 600 (1982).
19. L. Labriola *et al.*, *Mol. Cell. Endocrinol.* **264**, 16 (2007).
20. F. A. Scheeren *et al.*, *Nat. Immunol.* **6**, 303 (2005).
21. C. C. Chang, B. H. Ye, R. S. Chaganti, R. Dalla-Favera, *Proc. Natl. Acad. Sci. U.S.A.* **93**, 6947 (1996).
22. V. L. Seyfert, D. Allman, Y. He, L. M. Staudt, *Oncogene* **12**, 2331 (1996).
23. J. Miyazaki *et al.*, *Endocrinology* **127**, 126 (1990).
24. A. J. Weinhaus, N. V. Bhagroo, T. C. Brelje, R. L. Sorenson, *Endocrinology* **141**, 1384 (2000).
25. T. Shingo *et al.*, *Science* **299**, 117 (2003).
26. L. Scaglia, F. E. Smith, S. Bonner-Weir, *Endocrinology* **136**, 5461 (1995).
27. T. T. Yen *et al.*, *FASEB J.* **8**, 479 (1994).
28. J. C. Yao, *Best Pract. Res. Clin. Endocrinol. Metab.* **21**, 163 (2007).
29. We thank A. Yokoyama, G. Barsh, X. Hua, J. Hess, B. Cairns, L. Raetzman, A. Levine, and D. Bauer for helpful discussions and advice and members of the Kim laboratory for comments on the manuscript. Supported by a Kirschstein Postdoctoral Fellowship (S.K.K.); the Stanford Regenerative Medicine Training Program (H.C.); the Stanford Medical Scientist Training Program (J.J.H.); the American Diabetes Association (A.Y.Z. and J.J.H.); and NIH grant T32DK007217-32 (M.H.Y.). Work in the Kim laboratory was supported by a Stanford Cancer Council award, a gift from Raymond and Beverly Sackler, the Snyder Foundation, the NIH, the Juvenile Diabetes Research Foundation, and the Larry L. Hillblom Foundation.

Ordered Phosphorylation Governs Oscillation of a Three-Protein Circadian Clock

Michael J. Rust,[1]* Joseph S. Markson,[1,2]* William S. Lane,[3] Daniel S. Fisher,[4] Erin K. O'Shea[1]†

The simple circadian oscillator found in cyanobacteria can be reconstituted in vitro using three proteins—KaiA, KaiB, and KaiC. The total phosphorylation level of KaiC oscillates with a circadian period, but the mechanism underlying its sustained oscillation remains unclear. We have shown that four forms of KaiC differing in their phosphorylation state appear in an ordered pattern arising from the intrinsic autokinase and autophosphatase rates of KaiC and their modulation by KaiA. Kinetic and biochemical data indicate that one of these phosphoforms inhibits the activity of KaiA through interaction with KaiB, providing the crucial feedback that sustains oscillation. A mathematical model constrained by experimental data quantitatively reproduces the circadian period and the distinctive dynamics of the four phosphoforms.

Circadian clocks coordinate metabolism and behavior with diurnal cycles in the environment (*1*). These clocks traditionally have been understood as transcriptional feedback oscillators in which clock genes repress their own synthesis, creating negative feedback that drives oscillation (*1*). However, pioneering work by Kondo and colleagues has shown that the circadian clock of the cyanobacterium *Synechococcus elongatus* requires neither transcription nor translation (*2*), and circadian oscillations can be reconstituted in vitro using only three proteins: KaiA, KaiB, and KaiC (*3*).

KaiC is a hexameric enzyme (*4*) that can autophosphorylate (*5*) and autodephosphorylate (*6*) at both serine 431 (S431) and threonine 432 (T432) (*7*, *8*). The dimeric KaiA (*9*, *10*) enhances the autophosphorylation of KaiC (*11*), whereas KaiB antagonizes the activity of KaiA (*11*–*13*). In the absence of KaiA, KaiC fully dephospho-

[1]Howard Hughes Medical Institute, Faculty of Arts and Sciences Center for Systems Biology, Departments of Molecular and Cellular Biology and of Chemistry and Chemical Biology, Harvard University, Cambridge, MA 02138, USA. [2]Graduate Program in Biophysics, Harvard University, Cambridge, MA 02138, USA. [3]Microchemistry and Proteomics Analysis Facility, Faculty of Arts and Sciences Center for Systems Biology, Harvard University, Cambridge, MA 02138, USA. [4]Department of Applied Physics, Stanford University, Stanford, CA 94305, USA.

*These authors contributed equally to this work.
†To whom correspondence should be addressed. E-mail: erin_oshea@harvard.edu
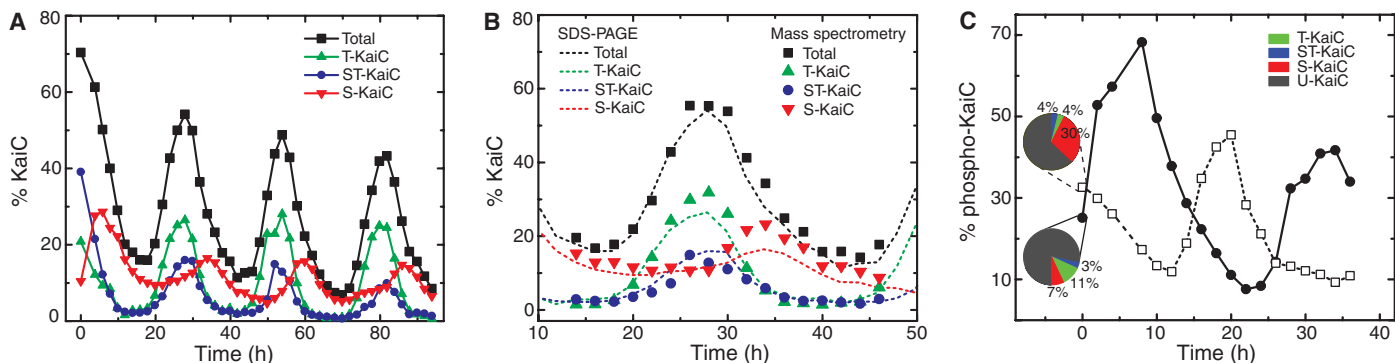
Fig. 1. Phosphorylation of KaiC is cyclically ordered. (**A**) Decomposition of total KaiC phosphorylation ("Total") into its constituent phosphoforms, measured by SDS-PAGE (used throughout this study unless noted otherwise). The percentage of U-KaiC (not shown) is equal to 100% − Total. See also fig. S10. (**B**) Comparison of phosphoform distributions measured by SDS-PAGE [dotted lines, from (A)] and by mass spectrometry (solid symbols). (**C**) The initial phosphoform distribution of KaiC determines the subsequent dynamics. We prepared KaiC enriched in T-KaiC (solid circles) by incubating unphosphorylated KaiC with epitope-tagged KaiA for 2.25 hours and then removing KaiA by immunoprecipitation. We prepared KaiC enriched in S-KaiC (open squares) by incubating unphosphorylated KaiC with epitope-tagged KaiA for 18 hours, removing KaiA, and then allowing KaiC to autodephosphorylate for 5.5 hours. In both cases, circadian oscillations were then initiated by adding KaiB, incubating for 1.5 hours, then reintroducing KaiA (*28*). Pie charts show the KaiC phosphoform distribution at the time of KaiA re-addition.

rylates (*9*). Complexes form between the Kai proteins (*14*), and the relative proportions of the KaiC-containing complexes oscillate (*9*, *15*).

The amount of phosphorylated KaiC oscillates with a circadian period (*11*). However, the total level of phosphorylation cannot be the only dynamical variable controlling the oscillator because it traverses the same value twice each day, but each time in a different direction (increasing during the subjective day and decreasing during the subjective night). Previous mathematical models have treated both phosphorylation sites as functionally equivalent (*16–24*) and have proposed additional dynamical variables arising from persistent conformational changes (*18*, *20–24*) or long-lived heterocomplexes (*16*, *17*); we hypothesized that additional variables could be found by examining the pattern of multisite phosphorylation of KaiC during the circadian cycle.

We measured the time dependence of phosphorylation at S431 and T432 by SDS–polyacrylamide gel electrophoresis (SDS-PAGE) (Fig. 1, A and B) and mass spectrometry (Fig. 1B), quantifying the four possible phosphorylation states: unphosphorylated (U-KaiC), phosphorylated only on S431 (S-KaiC), phosphorylated only on T432 (T-KaiC), and phosphorylated on both S431 and T432 (ST-KaiC). The concentration of each phosphoform oscillates with a circadian period but with different phases, creating an ordered pattern of phosphoform abundance during each cycle. Multisite phosphorylation of KaiC is required for oscillation, as point mutations at either S431 or T432 abolish rhythmicity (*7*, *8*) (fig. S1).

The predominance of distinct phosphoforms at different points in a cycle—T-KaiC during the phosphorylation phase and S-KaiC during the dephosphorylation phase—suggests that the phosphoform distribution (or a conformation tightly linked to the phosphorylation state) may determine the phase of the oscillator. If this is true, it should be possible to specify the initial phase by preparing KaiC with the appropriate phosphoform distri-
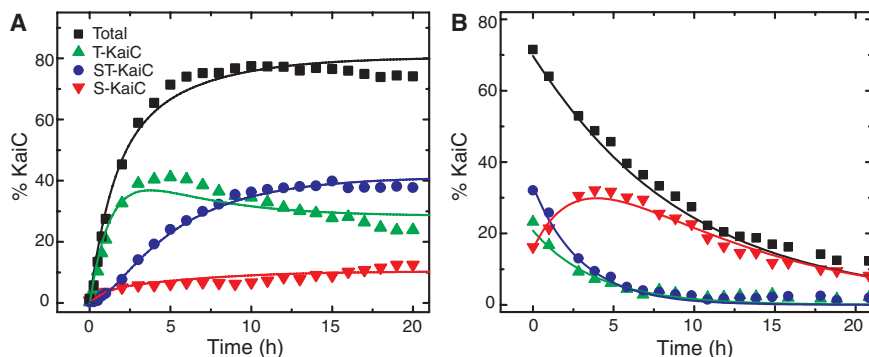

Fig. 2. KaiC phosphoform kinetics in partial reactions. (**A**) KaiC phosphorylation in the presence of KaiA. A least-squares fit (solid lines) to a four-state linear model (Fig. 2C) is shown. (**B**) Autonomous dephosphorylation of KaiC. Phosphorylated KaiC was prepared by incubation with KaiA, which was then removed by immunoprecipitation (*28*), initiating dephosphorylation. A least-squares fit (solid lines) to the same four-state model, with phosphorylation disallowed, is shown. (**C**) Reaction diagram for the four-state model with first-order kinetics.

bution and then adding KaiB and KaiA to initiate oscillations. Indeed, a reaction initiated with a KaiC pool enriched in T-KaiC begins in the phosphorylation phase, whereas a reaction initiated with high levels of S-KaiC begins in the dephosphorylation phase (Fig. 1C).

To investigate the origins of the ordered pattern of KaiC phosphoforms, we decomposed the oscillator into partial reactions. When KaiA is mixed with U-KaiC, T-KaiC accumulates first, followed by ST-KaiC, and eventually by S-KaiC (Fig. 2A). When highly phosphorylated KaiC is incubated alone, it autodephosphorylates, and the concentrations of T-KaiC and ST-KaiC decay monotonically (Fig. 2B). Concomitant with the decay of ST-KaiC, the abundance of S-KaiC transiently increases before eventually decaying, which suggests that S-KaiC is produced from ST-KaiC by dephosphorylation of T432. Neither the pattern of dephosphorylation nor its kinetics is

affected by the presence of KaiB (fig. S2). These data are described well by a linear model of KaiC phosphoform interconversion (Fig. 2C). Based on the rate constants calculated by fitting these data (Fig. 2, fig. S3, and table S1), we conclude that KaiA both promotes KaiC phosphorylation (according to a hyperbolic dependence quantified in fig. S4) (*11*) and inhibits some dephosphorylation steps (*6*). Phosphoform interconversions occur on the same time scale as the oscillations themselves, consistent with the idea that these are the key slow dynamical processes underlying the oscillator.

Combining the phosphoform dynamics observed in the partial reactions (Fig. 2, A and B) yields the same qualitative pattern of phosphoform abundance observed in the full oscillating reaction, suggesting that each cycle of the oscillator is composed of a phosphorylation phase of high KaiA activity followed by a dephosphorylation phase during which
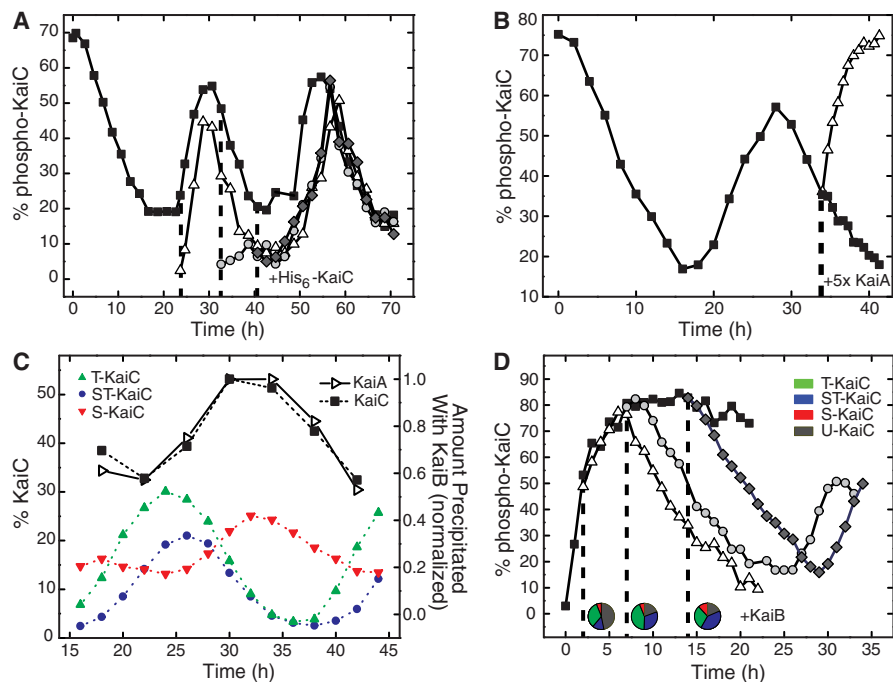
Fig. 3. KaiB suppresses KaiA activity in an S-KaiC dependent manner. (**A**) Global KaiA activity varies during the circadian cycle. Dephosphorylated His$_6$-KaiC (triangles, circles, diamonds) was added at 10% of the concentration of untagged KaiC (squares) at the indicated times. (**B**) Phosphorylation activity is rapidly restored by the addition of a five-fold excess of KaiA during the dephosphorylation phase (triangles), which continues in a control without excess KaiA (squares). (**C**) KaiB interaction with KaiC and KaiA scales with the abundance of S-KaiC. The right axis shows the normalized amounts of KaiC and KaiA that coimmunoprecipitate with KaiB-FLAG in an oscillating reaction; the left axis shows the corresponding phosphoform distribution. (**D**) KaiB does not affect phosphorylation until S-KaiC is abundant. Dephosphorylated KaiC was incubated with KaiA, and KaiB was introduced into the reaction at various time points (triangles, circles, diamonds) and compared to a control without added KaiB (squares). Pie charts show the KaiC phosphoform distribution at the time of KaiB addition.
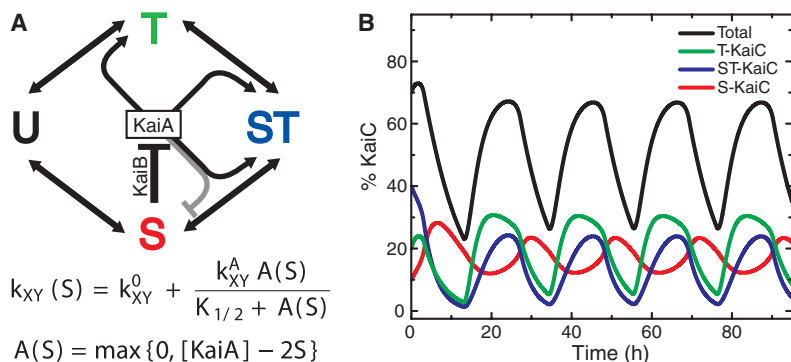
Fig. 4. A model for circadian oscillation driven by multisite KaiC phosphorylation. (**A**) KaiA activity alters the first-order rate constants for interconversion of KaiC phosphoforms. Lines emanating from KaiA ending in an arrowhead (black) or bar (gray) indicate stimulation or repression, respectively, of the transition toward the indicated form of KaiC. We show only the dominant effects (see table S2 and fig. S11). S-KaiC inactivates KaiA via KaiB. The interconversion rates from phosphoform X to Y, k_{XY}, depend hyperbolically on the concentration $A(S)$ of active KaiA monomers, which in turn depends on S-KaiC through its inhibitory activity. See the supporting online text for the complete equations of the dynamical model. (**B**) Numerical integration of the model reproduces circadian oscillation of KaiC phosphorylation.

KaiA is inactive. To test this idea, which has been proposed previously [e.g., (9)], we introduced a small quantity of epitope-tagged, dephosphorylated KaiC into the oscillator at various times (Fig. 3A); the tagged KaiC will phosphorylate only if KaiA is active. We observe KaiA activity only during the

phosphorylation phase. To rule out the alternative explanation that it is the sensitivity of KaiC to KaiA (21, 23)—rather than the activity of KaiA itself—that varies in a circadian cycle, we increased the concentration of KaiA in the middle of the dephosphorylation phase (Fig. 3B). The phosphorylation level of KaiC immediately increased, indicating that KaiC had not become insensitive to KaiA.

Inactivation of KaiA requires KaiB, as no oscillations occur in its absence (9) (Fig. 2A). Since previous studies have shown that KaiA-KaiB-KaiC complexes form during the clock reaction and that KaiB preferentially binds phosphorylated KaiC (9), we conjectured that inactivation of KaiA and hence initiation of the dephosphorylation phase occurs through a physical interaction between a specific phosphoform of KaiC and KaiA and KaiB. We found that the fraction of KaiC and KaiA complexed with KaiB closely follows the abundance of S-KaiC (Fig. 3C), which suggests that S-KaiC mediates a negative feedback loop through inactivation of KaiA via KaiB. Because S431 and T432 are buried within the KaiC oligomer (25), the specific preference of KaiB for S-KaiC suggests that changes in KaiC phosphorylation may be closely tied to conformational changes sensed by KaiB. To isolate the effects of phosphorylation at each site on KaiB-mediated feedback, we studied single-site nonphosphorylatable KaiC mutants and found that KaiB interacts preferentially with the mutant phosphorylatable only on S431 (fig. S1B) and also preferentially inhibits its phosphorylation (fig. S1A).

To further investigate the timing of KaiB function, we introduced it to a KaiA-KaiC reaction at various points (Fig. 3D). Adding KaiB early in the reaction, when S-KaiC levels are low, does not induce any measurable deviation from the KaiA-KaiC control until S-KaiC has reached ~10% abundance. In contrast, introduction of KaiB when S-KaiC levels are already high (~15%) rapidly induces dephosphorylation. Hence, S-KaiC plays a special role in promoting inactivation of KaiA. Indeed, the similarity between the dephosphorylation pattern caused by adding KaiB when S-KaiC levels are high and that induced by removing KaiA (fig. S5) demonstrates that adding KaiB in the presence of substantial S-KaiC is equivalent to removing KaiA.

To determine whether our understanding of the phosphoform kinetics and feedback mechanism can quantitatively account for the circadian oscillation of KaiC phosphorylation, we created a simple mathematical model (Fig. 4A and fig. S6A) constrained by our experimental measurements. The key assumptions of this minimal model are (i) the concentrations of the three phosphorylated species are the only slow dynamical variables; (ii) the interconversions between phosphoforms are first-order reactions with rates (table S2) that depend hyperbolically on the concentration of active KaiA (Fig. 4A and fig. S4); and (iii) each S-KaiC monomer (together with KaiB) inactivates one KaiA dimer. The phosphorylation and dephosphorylation rates are thus nonlinear functions of the concentration of

S-KaiC—the source of the crucial nonlinear feedback (Fig. 4A).

Using rate constants and a KaiA concentration dependence (table S2) derived solely from data on the non-oscillatory partial reactions (Fig. 2 and figs. S3 and S4), this simple model predicts (Fig. 4B) essential features of the circadian oscillator—period (~21 hours in the model), amplitude of total phosphorylation, sequential appearance of the phosphoforms, and the larger magnitude of the T-KaiC peak (see also fig. S7). This predictive ability suggests that the model captures the key elements of the in vitro oscillator. Modifying the model to explicitly treat the formation of KaiA-KaiC complexes (9) likely responsible for promoting KaiC phosphorylation makes it consistent with the observation that the oscillations are rather insensitive to the total concentration of Kai proteins (9) (supporting online text and fig. S8).

The following picture of the origin of stable oscillations emerges (fig. S6A). Starting from the unphosphorylated state, KaiA promotes phosphorylation that is kinetically favored at T432; subsequent phosphorylation at S431 produces ST-KaiC. ST-KaiC can decay via dephosphorylation of T432 to produce S-KaiC, but S-KaiC accumulation is slow because KaiA both inhibits that dephosphorylation and promotes rephosphorylation of S-KaiC to ST-KaiC. Thus, S-KaiC levels remain low until a substantial pool of ST-KaiC has formed. When S-KaiC levels do rise, KaiA activity is reduced, promoting dephosphorylation of ST-KaiC and thereby causing it to rapidly decay into S-KaiC. Thus, S-KaiC accelerates its own production (from ST-KaiC), which causes its concentration to overshoot the point at which KaiA is completely inactivated; this overshoot yields a reservoir of S-KaiC that permits extended inactivation of KaiA even as S-KaiC concentrations decrease through dephosphorylation. In the absence of KaiA activity, T-KaiC and ST-KaiC both dephosphorylate, and S-KaiC—which dephosphorylates more slowly—becomes the dominant remaining phosphorylated species. Eventually enough S-KaiC dephosphorylates for KaiA activity to return, and the cycle begins anew.

To focus on the essential slow dynamics and to be able to derive model parameters directly from our experimental data, our model ignores some known biochemical properties of the Kai proteins and abstracts others into the rate constants. KaiC exists as a hexamer (4), and we have neglected possible effects that depend on the state of the entire hexamer. Further, monomer exchange between hexamers (9) is not explicitly included, and we assume that inhibition of KaiA via KaiB occurs instantaneously upon formation of S-KaiC. In actuality, inhibition appears to take approximately 1 hour (fig. S9), possibly due to slow interaction between KaiB and KaiC or slow exchange of monomers between hexamers. These neglected effects have the potential to increase both the tendency of the system to oscillate and the amplitude of oscillation, but the success of our simplified model suggests that they are not part of the fundamental mechanism.

A recent report from the Kondo group (26) describes the differential phosphorylation of S431 and T432 during the circadian cycle and the interaction of KaiB with KaiC phosphorylated on S431. By using phosphomimetic KaiC mutants, they provide information about ordered phosphorylation complementary to and consistent with our kinetic study of wild-type KaiC.

The most striking behavior of the cyanobacterial circadian oscillator in vivo is its precision: Even with asynchronous cell division and an absence of external cues, the clock of a single cell and its offspring maintains precision to a small fraction of a day over several weeks (27). A reductive understanding of the various aspects of the clock—especially that of the core Kai oscillator presented here—should enable us to understand the effects of random fluctuations and variable environments. The Synechococcus clock provides an ideal model system for understanding how cells perform quantitative functions in highly variable intra- and extracellular environments.

References and Notes

1. S. L. Harmer, S. Panda, S. A. Kay, Annu. Rev. Cell Dev. Biol. 17, 215 (2001).
2. J. Tomita, M. Nakajima, T. Kondo, H. Iwasaki, Science 307, 251 (2005).
3. M. Nakajima et al., Science 308, 414 (2005).
4. T. Mori et al., Proc. Natl. Acad. Sci. U.S.A. 99, 17203 (2002).
5. T. Nishiwaki, H. Iwasaki, M. Ishiura, T. Kondo, Proc. Natl. Acad. Sci. U.S.A. 97, 495 (2000).
6. Y. Xu, T. Mori, C. H. Johnson, EMBO J. 22, 2117 (2003).
7. T. Nishiwaki et al., Proc. Natl. Acad. Sci. U.S.A. 101, 13927 (2004).
8. Y. Xu et al., Proc. Natl. Acad. Sci. U.S.A. 101, 13933 (2004).
9. H. Kageyama et al., Mol. Cell 23, 161 (2006).
10. S. Ye, I. Vakonakis, T. R. Ioerger, A. C. LiWang, J. C. Sacchettini, J. Biol. Chem. 279, 20511 (2004).
11. H. Iwasaki, T. Nishiwaki, Y. Kitayama, M. Nakajima, T. Kondo, Proc. Natl. Acad. Sci. U.S.A. 99, 15788 (2002).
12. S. B. Williams, I. Vakonakis, S. S. Golden, A. C. LiWang, Proc. Natl. Acad. Sci. U.S.A. 99, 15357 (2002).
13. Y. Kitayama, H. Iwasaki, T. Nishiwaki, T. Kondo, EMBO J. 22, 2127 (2003).
14. H. Iwasaki, Y. Taniguchi, M. Ishiura, T. Kondo, EMBO J. 18, 1137 (1999).
15. H. Kageyama, T. Kondo, H. Iwasaki, J. Biol. Chem. 278, 2388 (2003).
16. S. Clodong et al., Mol. Syst. Biol. 3, 90 (2007).
17. E. Emberly, N. S. Wingreen, Phys. Rev. Lett. 96, 038303 (2006).
18. G. Kurosawa, K. Aihara, Y. Iwasa, Biophys. J. 91, 2015 (2006).
19. A. Mehra et al., PLoS Comput. Biol. 2, e96 (2006).
20. F. Miyoshi, Y. Nakayama, K. Kaizu, H. Iwasaki, M. Tomita, J. Biol. Rhythms 22, 69 (2007).
21. T. Mori et al., PLoS Biol. 5, e93 (2007).
22. H. Takigawa-Imamura, A. Mochizuki, J. Biol. Rhythms 21, 405 (2006).
23. J. S. van Zon, D. K. Lubensky, P. R. Altena, P. R. ten Wolde, Proc. Natl. Acad. Sci. U.S.A. 104, 7420 (2007).
24. M. Yoda, K. Eguchi, T. P. Terada, M. Sasai, PLoS ONE 2, e408 (2007).
25. R. Pattanayek et al., Mol. Cell 15, 375 (2004).
26. T. Nishiwaki et al., EMBO J. 26, 4029 (2007).
27. I. Mihalcescu, W. Hsing, S. Leibler, Nature 430, 81 (2004).
28. Materials and methods are available as supporting material on Science Online.
29. We thank B. Budnik, J. Neveu, and R. Robinson for assistance with mass spectrometry; T. Mori and C. Johnson for SDS-PAGE conditions for phosphoform separation; J. Ferrell for helpful discussions; and B. Stern, R. Losick, M. Ebert, S. Douglas, and T. Schmidt for comments on the manuscript. This work was supported by an NSF Graduate Research Fellowship (J.S.M.), NSF grant DMR-0229243 (D.S.F.), and the Howard Hughes Medical Institute (E.K.O.).

Disentangling Genetic Variation for Resistance and Tolerance to Infectious Diseases in Animals

Lars Råberg,[1,2]* Derek Sim,[1]† Andrew F. Read[1]†

Hosts can in principle employ two different strategies to defend themselves against parasites: resistance and tolerance. Animals typically exhibit considerable genetic variation for resistance (the ability to limit parasite burden). However, little is known about whether animals can evolve tolerance (the ability to limit the damage caused by a given parasite burden). Using rodent malaria in laboratory mice as a model system and the statistical framework developed by plant-pathogen biologists, we demonstrated genetic variation for tolerance, as measured by the extent to which anemia and weight loss increased with increasing parasite burden. Moreover, resistance and tolerance were negatively genetically correlated. These results mean that animals, like plants, can evolve two conceptually different types of defense, a finding that has important implications for the understanding of the epidemiology and evolution of infectious diseases.

Defense against pathogenic microorganisms and other parasites can be divided into two conceptually different components: resistance (the ability to limit parasite burden) and tolerance (the ability to limit the disease severity induced by a given parasite burden) (1–4). It is important to distinguish between these two components because, by definition, resistance has a negative effect on